Journal of the Korean Crystal Growth and Crystal Technology
Vol. 31, No. 2 (2021) 96-101
https://doi.org/10.6111/JKCGCT.2021.31.2.096

p-ISSN 1225-1429
e-ISSN 2234-5078

Electrocatalytic properties of Te incorporated $Ni(OH)_2$ microcrystals grown on Ni foam

Jung-Il Lee[*,**], Seong Gyun Oh[*], Yun Jeong Kim[*], Seong Ju Park[*], Gyoung Seon Sin[*], Ji Hyeon Kim[*] and Jeong Ho Ryu[*,**,†]

*Department of Materials Science and Engineering, Korea National University of Transportation, Chungju 27469, Korea
**Energy Fusion Technology Laboratory, Korea National University of Transportation, Chungju 27469, Korea

(Received March 25, 2021)
(Revised April 2, 2021)
(Accepted April 2, 2021)

Abstract Developing effective and earth-abundant electrocatalyst for oxygen evolution reaction (OER) and hydrogen evolution reaction (HER) is critical for the commercialization of a water splitting system. In particular, the overpotential of the OER is relatively higher than the HER, and thus, it is considered that one of the important methods to enhance the performance of the electrocatalyst is to reduce the overpotential of the OER. We report effects of incorporation of metalloid into $Ni(OH)_2$ microcrystal on electrocatalytic activities. In this study, Te incorporated $Ni(OH)_2$ (χTe-$Ni(OH)_2$) were grown on three-dimensional porous NF by a facile solvothermal method with $\chi = 1$, 3 and 5. Homogeneous microplate structure on the NF was clearly observed for the $Ni(OH)_2$/NF and χTe-$Ni(OH)_2$/NF samples. However, irregular and collapsed nanostructures were found on the surface of nickel foam when Te precursor ratio is (χ) over 3. Electrocatalytic OER properties were analysed by Linear sweep voltammetry (LSV) and Electrochemical impedance spectroscopy (EIS). The amount of Te incorporation used in the electrocatalytic reaction was found to play a crucial role in improving catalytic activity. The optimum Te amount (χ) introduced into the $Ni(OH)_2$/NF was discussed with respect to their OER performance.

Key words Elecrocatalysis, $Ni(OH)_2$ microcrystals, Water splitting, OER

1. Introduction

Water splitting is one of efficient methods to produce clean hydrogen, which can be utilized as an alternative energy for traditional fossil fuels [1,2]. Water electrolysis process contains anodic oxygen evolution reaction (OER) and cathodic hydrogen evolution reaction (HER) [3,4]. The slow kinetic process of OER on the anode always leads to a high overpotential, which would decrease the efficiency of water splitting and result in a slow-going hydrogen production rate on the cathode. Even some noble metal materials such as ruthenium/iridium oxides (RuO_2/IrO_2) have been proved to be efficient catalysts for OER [5], their large-scale commercialization is limited due to their high cost and low production. Therefore, development of efficient and cheap OER electrocatalysts is extremely necessary for the hydrogen production through water electrolysis [6].

In the past decade, Ni-based catalysts, specially oxides, hydroxides, chalcogenides and others have been applied for OER due to their highly active and low-cost properties [7]. In order to address the corrosion issue under harsh alkaline environment and increase the reactive areas of Ni-based catalysts [8], the coupling of Ni nanoparticles with carbon materials has become an effective way [9]. Additionally, heteroatom doping in composite catalyst could ulteriorly modify the electron transfer [10]. However, the increased structural complexity would gain difficulty in mechanism analysis for this kind of catalysts. In this case, in-situ techniques along with other effective characterizations becomes strongly needed to better understand the catalytic roles of different parts and mechanism. Here, we synthesized three-dimensional (3D) porous nickel foam with $Ni(OH)_2$ microcrystals via facile solvothermal route.

In this study, we show that metalloid incorporation into $Ni(OH)_2$ microcrystals can be a promising strategy for designing highly efficient and commercial electrocatalysts for alkaline OER. Tellurium (Te) was selected as a promising metalloid element for modulating the catalytic properties of nickel oxide microstructure, where electrical conductivity and number of active sites can be simultaneously enhanced [11]. To the best of our knowledge, metalloid incorporation for tuning electrocatalytic properties of $Ni(OH)_2$ has rarely been studied despite of

†Corresponding author
E-mail: jhryu@ut.ac.kr

its high potential. Encouraged by the above discussion, we introduced Te into the $Ni(OH)_2$ microcrystals grown on three-dimensional porous nickel foam (NF) by a facile solvothermal method. Benefiting from the optimized electronic structure from the introduced Te and the conductive NF as the current collector, the $Ni(OH)_2$ microcrystals on NF displays superior OER performance. Optimum Te amount introduced into the $Ni(OH)_2$ microcrystals was discussed on the electrocatalytic OER performance.

2. Experimental

2.1. Growth of $Ni(OH)_2$ and χTe-$Ni(OH)_2$ nanoplate on nickel foam

Nickel foam (NF) was treated with acetone and then with 3 M HCl solution for 10 min using ultrasonication cleaner. The cleaned NF was dried overnight. All the chemicals were purchased from Kojundo chemical and were directly used without further purification. For the synthesis of $Ni(OH)_2$ microcrystal, as-prepared NF was immersed in 20 ml of deionized (DI) water. Then, the resulting solution was transferred to Teflon-lined autoclave and hydrothermally reacted at 180°C for 5 h. The $Ni(OH)_2$ microcrystals on NF sample was washed several times with DI water. The final $Ni(OH)_2$ microcrystals grown on NF sample ($Ni(OH)_2$/NF) was subsequently dried in vacuum at 60°C for overnight. Synthesis method for χTe-$Ni(OH)_2$ on NF samples (χTe-$Ni(OH)_2$/NF) were same as that of $Ni(OH)_2$/NF, except that tellurium tetrachloride ($TeCl_4$) solution was added before hydrothermal reaction. The added $TeCl_4$ solution concentration in the χTe-$Ni(OH)_2$ were 1.0, 3.0 and 5.0×10^{-3} mol for the χ = 1, 3, 5, respectively.

2.2. Characterizations

Microstructural images of each samples were observed by field emission scanning electron microscopy (FE-SEM; model S4800; Hitachi) equipped with energy dispersive X-ray (EDX). X-ray diffraction (XRD) was performed using a D/MAX-2500/PC (Rigaku) diffractometer at 40 kV and 100 mA with Cu-Kα radiation (λ = 0.15418 nm). The electrochemical properties of catalysts in 1 M KOH were tested using a three-electrode electrochemical cell controlled by an electrochemistry workstation (model Autolab PGSTAT; Metrohm), in which the catalyst grown on NF was used directly as the working electrode [12]. Prior to measurements, the electrolyte (1 M KOH, pH 13.7) was purged for about 10 min with O_2, and the working electrodes were sealed on all edges with a custom-made acrylate adhesive except for the working surface area of 0.25 cm^2. Graphite rod and $Hg|Hg_2SO_4$ were used as the counter and reference electrodes, respectively. A titration vessel of clear glass was used as a testing cell. The distance between working and reference electrodes was close to 1 cm. Linear sweep voltammetry (LSV) was measured with a scan rate of 0.5 mV/s in a range from 1.23 to 1.9 V vs. a reversible hydrogen electrode (RHE). Applied potential values were calibrated against RHE, and all polarization curves were *iR*-corrected. Electrochemical impedance spectroscopy (EIS) measurement was conducted over the frequency range of 0.1-100 kHz at 1.45 V_{RHE} with a sinusoidal amplitude of 5 mV.

3. Results and Discussion

$Ni(OH)_2$/NF exhibits poor electrical conductivity, which impedes facile charge transfer between the surface of catalyst and the adsorbed reactant. After Te incorporation, electrical properties of χTe-$Ni(OH)_2$/NF can be significantly improved to easily take up electrons in hydroxyl ions, crucially accelerating water oxidation kinetics. Te element can be incorporated into the transition metal that is, a real catalytic active site in $Ni(OH)_2$/NF, where a strong covalent p-d hybridization occurred with a highly polarized local electronic structure significantly accelerating electrocatalytic OER activity of χTe-$Ni(OH)_2$/NF samples [13].

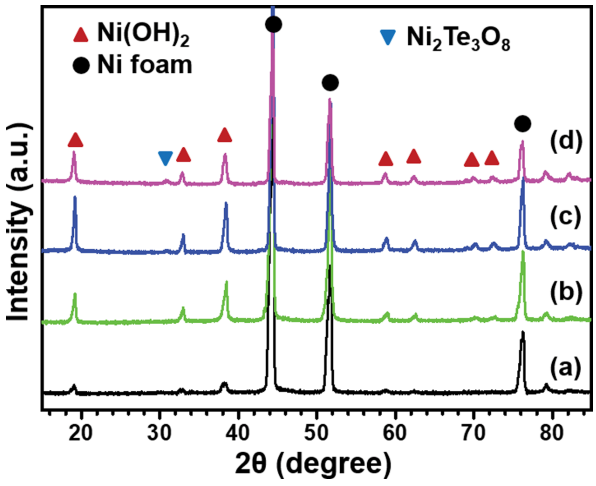

Fig. 1. XRD patterns of the (a) $Ni(OH)_2$/NF, (b) Te-$Ni(OH)_2$/NF, (c) 3Te-$Ni(OH)_2$/NF, and (d) 5Te-$Ni(OH)_2$/NF samples.

$Ni(OH)_2$/NF and χTe-$Ni(OH)_2$/NF microcrystals were synthesized by direct growth of NF using tellurium chloride via hydrothermal reaction at 180°C for 5 h. Typical XRD analysis confirmed the formation of the $Ni(OH)_2$/NF and χTe-$Ni(OH)_2$/NF crystal structures as shown in Fig. 1. The strong diffraction peaks near 44° and 51° could be assigned to Ni metal in the NF substrate. The XRD patterns revealed the crystal structure and phase purity of the $Ni(OH)_2$/NF microcrystals. Except for the peaks from the NF substrate, all other detectable diffraction peaks at low 2θ angles could be indexed to the theophrastite-like β-$Ni(OH)_2$ phase (PDF 00-059-0462). Prominent diffraction peaks for the layered nickel-cobalt hydroxide were observed from at 19°, 33° and 38°. Notably, secondary phase related to Te ($Ni_2Te_3O_8$) was observed at 31° in the XRD pattern of the 5Te-$Ni(OH)_2$/NF sample, indicating that a very high Te content is not desirable for synthesizing Te-incorporated transition metal hydroxide nanosheets on the NF substrate.

Fig. 2 shows highly magnified FE-SEM images for the $Ni(OH)_2$/NF and χTe-$Ni(OH)_2$NF (χ = 1, 3, 5) microcrystals. Fig. 2 represents that large-scale highly interconnected and aligned microplate structure vertically grow on the skeletons of the NF with uniform morphology and dense loading, forming an ordered and 3D network with a highly open and interstitial structure. Homogeneous microplate structure on the 3D macroporous NF was clearly observed for the $Ni(OH)_2$/NF and χTe-$Ni(OH)_2$/NF (χ = 1, 3) microcrystals. However, when the Te adding amount (χ) is over 3, irregular and collapsed microstructure were found on the surface of $Ni(OH)_2$ microcrystals. Also, highly aggregated particle morphology with the large area of bare nickel foam, uncovered by the grown material, was formed for when Te precursor ratio further increased to more than χ = 3 as shown in Fig. 2(d).

The electrocatalytic activities of $Ni(OH)_2$/NF and χTe-$Ni(OH)_2$/NF samples were tested in alkaline media (1 M KOH aqueous solution) using a three-electrode system. Linear sweep voltammetry (LSV) was performed at a scan rate of 0.5 mV/s on the samples. NF substrates were directly used as working electrodes, while a rotating disk electrode (RDE) was employed for testing powder samples such as RuO_2. To remove the bubbles generated during measurement, the RDE was continu-

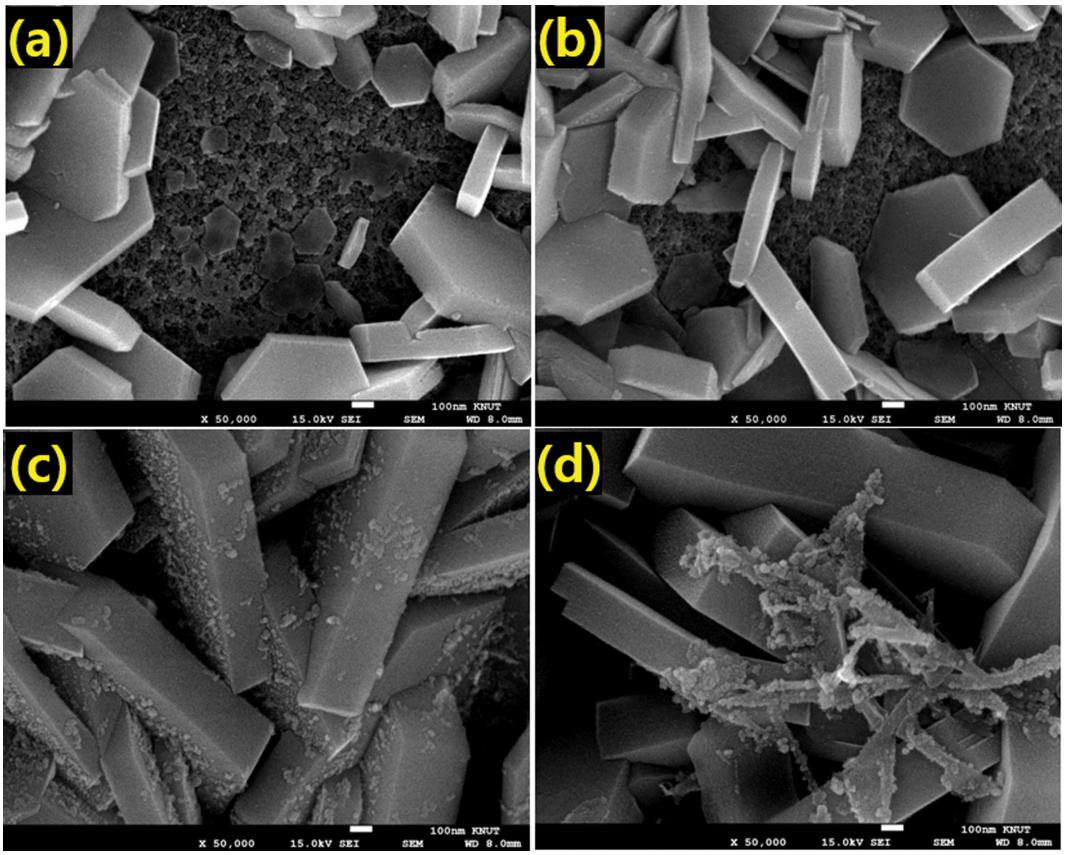

Fig. 2. Highly magnified FE-SEM images for the (a) $Ni(OH)_2$/NF, (b) Te-$Ni(OH)_2$/NF, (c) 3Te-$Ni(OH)_2$/NF and (d) 5Te-$Ni(OH)_2$/NF samples.

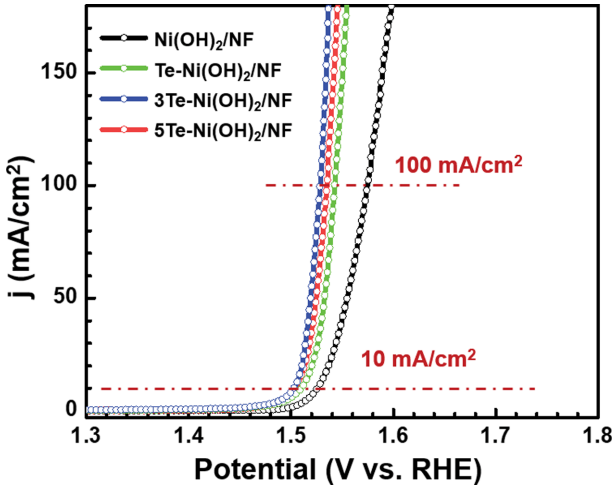

Fig. 3. LSV curves at a scan rate of 0.5 mV/s for electrocatalytic OER properties of the $Ni(OH)_2$/NF and χTe-$Ni(OH)_2$/NF samples.

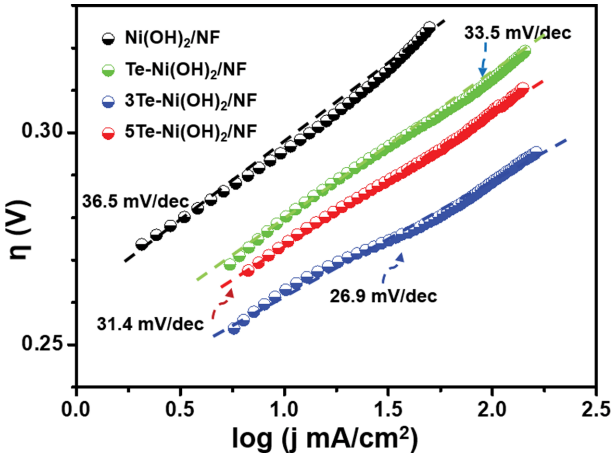

Fig. 4. Tafel slopes of $Ni(OH)_2$/NF and χTe-$Ni(OH)_2$/NF samples derived from the measured LSV curves.

ously rotated at 2,000 rpm. All measured potentials were *iR*-compensated and were then referenced to the reversible hydrogen electrode (RHE). Notably, χTe-$Ni(OH)_2$/NF exhibited enhanced catalytic activity for water oxidation compared to $Ni(OH)_2$/NF sample. The overpotential (η) required to transmit a current density of 10 mA/cm^2 (η^{10}) is conventionally used as a standard to compare electrocatalytic OER performance [14].

Fig. 3 shows LSV curves with a scan rate of 0.5 mV/s for electrocatalytic OER properties of the $Ni(OH)_2$/NF and χTe-$Ni(OH)_2$/NF samples. The η^{10} substantially decreased when Te was introduced into $Ni(OH)_2$/NF. The 3Te-$Ni(OH)_2$/NF sample required an η^{10} of 270 mV, while η^{10} for $Ni(OH)_2$/NF was about 295 mV as shown in Fig. 3. Importantly, an overpotential of only 285 mV was needed for 3Te-$Ni(OH)_2$/NF to generate a high current density of 100 mA/cm^2, compared to the 330 mV for the $Ni(OH)_2$/NF sample, which can be beneficial for practical electrolysis applications. The amount of Te incorporation used in the reaction was found to play a crucial role in improving catalytic activity. In terms of overpotential, the Te content in 3Te-$Ni(OH)_2$/NF resulted in the best catalytic activity for water oxidation. However, further increasing Te content to 5Te-$Ni(OH)_2$/NF significantly disturbed its catalytic activity, which may be related to secondary phase observed in Fig. 1(d), and irregular microcrystal growth on the nickel foam substrate as shown in Fig. 2(d).

Tafel plots of the samples were derived from the measured LSV curves based on the Tafel equation ($\eta = b \times \log j + a$), where χ is the overpotential, j is the current density, and b is the Tafel slope. Tafel slopes of $Ni(OH)_2$/NF and χTe-$Ni(OH)_2$/NF were calculated and represented in Fig. 4. The measured Tafel slopes of the $Ni(OH)_2$/NF was 36.5 and the and χTe-$Ni(OH)_2$/NF were 33.5, 26.9 and 31.4 mV/dec for the χ values of 1, 3, and 5, respectively. Among the samples, 3Te-$Ni(OH)_2$/NF exhibited the smallest Tafel slope (26.9 mV/dec) compared to $Ni(OH)_2$/NF (36.5 mV/dec), highlighting the potential use of Te-$Ni(OH)_2$/NF for industrial electrolyzer because a smaller Tafel slope is desirable to reduce power losses [15].

Charge transfer resistance (R_{ct}) between electrocatalysts and electrolytes can be obtained from the semicircle diameter in the high-frequency region of a Nyquist plot (Z′ vs. −Z″) measured by electrochemical impedance spectroscopy (EIS). Here, the smaller diameter generally represents the lower R_{ct}. Fig. 5 represents the EIS data of the samples, where χTe-$Ni(OH)_2$/NF sam-

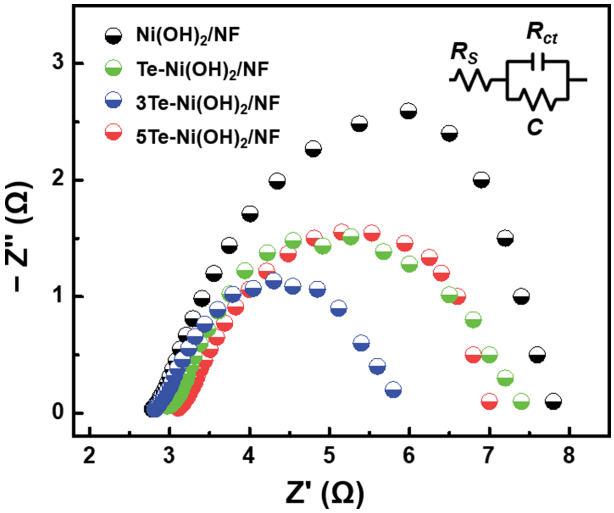

Fig. 5. EIS data of the $Ni(OH)_2$/NF and χTe-$Ni(OH)_2$/NF samples.

ples (6.0~7.5 Ω) showed a value of R_{ct} that was obviously lower than that of the $Ni(OH)_2$/NFsample (~8.0 Ω). Notably, 3Te-$Ni(OH)_2$/NF exhibited a minimum R_{ct} (~6.0 Ω), implying the significant role of Te incorporation for facilitating charge transfer from the catalyst surface to the adsorbed chemical reactants. Further increasing Te content (5Te-$Ni(OH)_2$/NF) increased its charge transfer resistance, which may be related to poorly grown nanosheets on the nickel foam substrate, which is same result with LSV curve and Tafel slope.

To quantitatively evaluate catalytic activity of $Ni(OH)_2$/NF and χTe-$Ni(OH)_2$/NF samples, we first estimated the double-layer capacitance (C_{dl}) using a CV method in the non-Faradaic region where the current generated from electrical double layer charging is essentially related to electrochemical surface area (ECSA). The CV test was conducted in an O_2-saturated 1 M KOH solution to estimate the C_{dl} at non-Faradaic overpotentials. CV measurements were performed at various scan rates (20, 40, 60, 80, 100, and 120 mV/s). The difference in current density between the anodic and cathodic sweeps ($J_{anodic} - J_{cathodic}$) at the middle of potential range was plotted as a function of the scan rate, where the slope has a linear relationship with twice the C_{dl} of the catalyst [16]. The C_{dl} was calculated to be 40.18 mF for 3Te-$Ni(OH)_2$/NF sample, while $Ni(OH)_2$/NF and 5Te-$Ni(OH)_2$/NF exhibited much lower C_{dl} values of 17.95 and 31.50 mF/cm^2, respectively as shown in Fig. 6.

For quantitative analysis of the catalytic activity of the samples, the turnover frequency (TOF) needs to be calculated as $TOF = j \times A/(4 \times F \times N_s)$, where j is the current density (A/cm^2) at a specific overpotential, A is the electrode area (cm^2), F is the Faraday constant (96,485

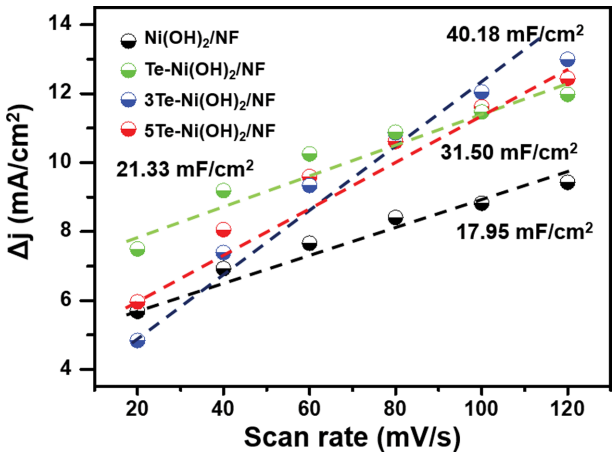

Fig. 6. The current difference between anodic and cathodic sweeps as a function of scan rate. The slope of the fitted line was used to calculate C_{dl}.

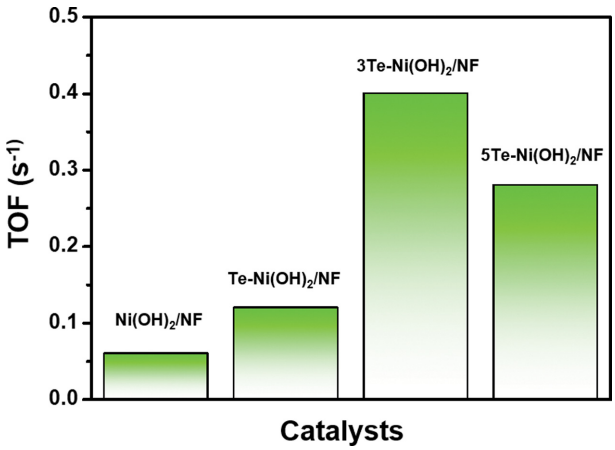

Fig. 7. TOFs of the $Ni(OH)_2$/NF and χTe-$Ni(OH)_2$/NF samples at an overpotential of 290 mV.

C/mol), and N_s is the concentration of active sites (mol/cm^2). Cyclic voltammetry (CV) was performed to calculate N_s for the redox reactions at different scan rates in 1.0 M KOH electrolyte. The peak currents were plotted verses scan rates where the slope is equal to, $Slope = n^2F^2AN_s/4RT$, here n is the amount of electrons transferred (here n = 1), F presents Faradic constant, A is the surface area of the electrode, Ns is the surface concentration of active sites (mol/cm^2), R and T are the ideal gas constant and the absolute temperature, respectively [11]. The TOF value of 3Te-$Ni(OH)_2$/NF was 0.4 s^{-1} at an overpotential of 290 mV, which is much higher than those of $Ni(OH)_2$/NF (0.06 s^{-1}) and 5.0Te-$Ni(OH)_2$/NF (0.28 s^{-1}) as shown in Fig. 7, indicating the intrinsically high catalytic activity of 3Te-$Ni(OH)_2$/NF sample.

4. Summary

In summary, Te-incorporated nickel oxide microcrystals were developed as highly efficient and low-cost electrocatalysts for water oxidation under alkaline conditions. The $Ni(OH)_2$ and χTe-$Ni(OH)_2$ (χ = 1, 3, 5) microcrystals were successfully grown on nickel foam (NF) via hydrothermal reaction at 180°C for 5 h. Homogeneous nanoplate structure on the NF was clearly observed for the $Ni(OH)_2$/NF and χTe-$Ni(OH)_2$/NF samples. When Te ratio (χ) is higher over 3, irregular and collapsed nanostructures were found on the surface of NF. The electrocatalyst of 3Te-$Ni(OH)_2$/NF sample provided current densities of 10 and 100 mA/cm^2 at overpotentials of only 270 and 285 mV, respectively, with a very small Tafel slope of 26.9 mV/dec in an alkaline medium. Moreover, 3Te-$Ni(OH)_2$/NF exhibited a minimum R_{ct}

(~6 Ω) wiht respect to the $Ni(OH)_2$/NF sample (~8 Ω), implying the significant role of Te incorporation for facilitating charge transfer from the catalyst surface to the adsorbed chemical reactants. The double layer capacitance C_{dl} was calculated to be 40.18 mF for 3Te-$Ni(OH)_2$/NF compared to the value of 17.95 for $Ni(OH)_2$/NF. The 3Te-$Ni(OH)_2$/NF sample showed much higher TOF compared to the $Ni(OH)_2$/NF and other χTe-$Ni(OH)_2$ samples. These results demonstrate that the χTe-$Ni(OH)_2$/NF are promising electrocatalysts for water oxidation and optimum Te incorporation content (χ) is 3.

Acknowledgement

This research was supported by the Basic Science Research Program through the National Research Foundation of Korea (NRF) funded by the Ministry of Education (No. 2019R1I1A3A0106266212).

References

[1] B. You and Y. Sun, "Innovative strategies for electrocatalytic water splitting", Acc. Chem. Res. 51 (2018) 1571.
[2] Y. Shi and B. Zhang, "Recent advances in transition metal phosphide nanomaterials: synthesis and applications in hydrogen evolution reaction", Chem. Soc. Rev. 45 (2016) 1529.
[3] M. Zeng and Y. Li, "Recent advances in heterogeneous electrocatalysts for the hydrogen evolution reaction", J. Mater. Chem. A 3 (2015) 14942.
[4] H.J. Lee, K. Cho and J.H. Ryu, J. Korean Cryst. Growth Cryst. Technol. 30 (2020) 17.
[5] W. Zhang, W. Wang, H. Shi, Y. Liang, J. Fu and M. Zhu, "Surface plasmon-driven photoelectrochemical water splitting of aligned ZnO nanorod arrays decorated with loading-controllable au nanoparticles", Sol. Energy Mater. Sol. Cells 180 (2018) 25.
[6] R. Kant, S. Pathak and V. Dutta, "Design and fabrication of sandwich-structured αFe_2O_3/Au/ZnO photoanode for photoelectrochemical water splitting, Sol. Energy Mater. Sol. Cells 178 (2018) 38.
[7] S.A. Shah, Z. Ji, X. Shen, X. Yue, G. Zhu, K. Xu, A. Yuan, N. Ullah, J. Zhu, P. Song and X. Li, "Thermal synthesis of FeNi@nitrogen-doped graphene dispersed on nitrogendoped carbon matrix as an excellent electrocatalyst for oxygen evolution reaction", ACS Appl. Energy Mater. 2 (2019) 4075.
[8] T. Zhang, M.-Y. Wu, D.-Y. Yan, J. Mao, H. Liu, W.-B. Hu, X.-W. Du, T. Ling and S.-Z. Qiao, "Engineering oxygen vacancy on NiO nanorod arrays for alkaline hydrogen evolution", Nano Energy 43 (2018) 103.
[9] L. Lin, T. Liu, B. Miao and W. Zeng, "Hydrothermal fabrication of uniform hexagonal NiO nanoshet: Structure, growth and response", Mater. Lett. 102-103 (2013) 43.
[10] G.-Q. Han, Y.-R. Liu, W.-H. Hu, B. Dong, X. Li, X. Shang, Y.-M. Chai, Y.-Q. Liu and C.-G. Liu, "Three dimensional nickel oxides/nickel structure by in situ electro-oxidation of nickel foam as robust electrocatalyst for oxygen evolution reaction", Appl. Surf. Sci. 359 (2015) 172.
[11] H. Han, K.M. Kim, J.H. Ryu, H.J. Lee, J. Woo, G. Ali, K.Y. Chung, T. Kim, S. Kang, S. Choi, J. Kwon, Y.-C. Chung, S. Mhin and T. Song, "Boosting oxygen evolution reaction of transition metal layered double hydroxide by metalloid incorporation", Nano Energy 75 (2020) 104945.
[12] M. Xu and M. Wei, "Layered double hydroxide-based catalysts: Recent advances in preparation, structure, and applications", Adv. Funct. Mater. 28 (2018) 1802943.
[13] J. Masa, I. Sinev, H. Mistry, E. Ventosa, M. de la Mata, J. Arbiol, M. Muhler, B. Roldan Cuenya and W. Schuhmann, "Ultrathin high surface area nickel boride (NixB) nanosheets as highly efficient electrocatalyst for oxygen evolution", Adv. Energy Mater. 7 (2017) 1700381.
[14] C.C.L. McCrory, S. Jung, J.C. Peters and T.F. Jaramillo, "Benchmarking heterogeneous electrocatalysts for the oxygen evolution reaction", J. Am. Chem. Soc. 135 (2013) 16977.
[15] N.T. Suen, S.F. Hung, Q. Quan, N. Zhang, Y.J. Xu and H.M. Chen, "Electrocatalysis for the oxygen evolution reaction: Recent development and future perspectives", Chem. Soc. Rev. 46 (2017) 337.
[16] X. Du, J. Huang, J. Zhang, Y. Yan, C. Wu, Y. Hu, C. Yan, T. Lei, W. Chen, C. Fan and J. Xiong, "Modulating electronic structures of inorganic nanomaterials for efficient electrocatalytic water splitting", Angew. Chem. Int. Ed. 58 (2019) 4484.